Pergamon

Int. J. Heat Mass Transfer. Vol. 41, No. 10, pp. 1139–1148, 1998

Printed in Great Britain
0017–9310/98 $19.00 + 0.00

PII: S0017–9310(97)00250–0

Unsteady heat transfer and velocity of a cylinder in cross flow— I. Low freestream turbulence

J. W. SCHOLTEN and D. B. MURRAY
Department of Mechanical Engineering, Trinity College, Dublin 2, Ireland

(*Received* 22 *January* 1997 *and in final form* 21 *August* 1997)

Abstract—This paper is the first of two papers which describe simultaneous measurements of time resolved heat flux and local velocity at the surface of a cylinder in cross flow. Time-averaged Nusselt numbers, heat flux auto spectra and time traces are presented and the coherence and phase difference between the velocity and heat flux signals are used to establish that the heat transfer fluctuations at the front of the cylinder originate in pulsation of the flow field resulting from vortex shedding in the wake. The effect of increased levels of freestream turbulence on the heat transfer fluctuations is explored in Part II of this study. © 1998 Elsevier Science Ltd.

INTRODUCTION

Studies of heat transfer from cylinders in cross flow have been widely reported. Examples are reviews by Morgan [1] on average heat transfer rates from single cylinders in cross flow and by Zukauskas and Ziugzda [2] on the local heat transfer characteristics of tubes in cross flow. The results of these studies are, however, limited to time averaged Nusselt numbers whereas time resolved heat transfer information is more useful for the identification of convective heat transfer mechanisms. For example, studies by Murray and Fitzpatrick [3] and Scholten and Murray [4] of convective heat transfer in gas-particle cross flows have suggested that measured local reductions in heat transfer may result from turbulence suppression by the particles. In the absence of instantaneous local heat transfer measurements, it is not possible to establish definitively the role of turbulence modification in particulate heat transfer applications.

Measurements of unsteady heat transfer from cylinders in cross flow are difficult to obtain, due to the high frequency and small amplitude of the random fluctuations encountered. Fluctuations in heat transfer for an oscillating cylinder in cross flow were measured by Rosicskowski and Hollworth [5], but this study was limited to the low frequencies associated with the oscillations. Likewise, for cylinders immersed in gas fluidised beds, the studies of George [6], Katoh *et al.* [7] and Rottger and Renz [8] have all examined the instantaneous local heat transfer characteristics. Again, the frequencies under consideration are linked to bubble motion and particle contact at the surface and are significantly lower than encountered in turbulent cross flows. For a cylinder in a cross flow of high turbulence intensity, Simmons *et al.* [9] and Ching and O'Brien [10] have recorded fluctuations in the heat transfer rates from measurements around the front stagnation point. No results were reported for the full cylinder circumference. The fluctuating flow field around cylinders has also been studied extensively. For example, Meyer and Larsen [11] and Balabani and Yianneskis [12] used laser Doppler anemometry to investigate the mean flow and turbulence structure for flows through tube arrays. However, the data have not been correlated with fluctuating heat transfer measurements.

This paper describes a study in which time resolved heat flux is measured locally, using a hot film, on the surface of a cylinder in cross flow. Because of the influence of fluid velocity on convection, a better understanding of convective heat transfer mechanisms can be achieved through combining unsteady measurements of velocity and heat flux. Thus, local velocity close to the surface is measured simultaneously, using a laser Doppler anemometer. Reynolds numbers corresponding to laminar boundary layer development are used. The heat transfer results are presented in the form of auto spectra and time traces, in addition to the variation in time averaged Nusselt numbers around the circumference. From the simultaneous measurements, the coherence and phase difference between the velocity and heat flux signals are examined, with a view to determining the origin of the surface heat transfer fluctuations.

EXPERIMENTAL SET-UP AND INSTRUMENTATION

The test facilities consist of a low turbulence wind tunnel ($Tu \cong 0.5\%$) with a perspex test section of 127 mm × 127 mm. (A summary of the mainstream turbulence intensities, measured with a hot wire probe upstream of the test cylinder, is given in Table 1 for the range of velocities used in these tests.) The test cylinder was installed horizontally in this section and

NOMENCLATURE

A_{eff}	effective surface area of the hot film sensor
D	diameter of the test cylinder
k_{air}	conductivity of air
k_{kapton}	conductivity of kapton substrate
Nu	Nusselt number
Nu_{fsp}	Nusselt number at front stagnation point
Nu_m	circumferentially averaged Nusselt number
q_{cond}	conductive heat flux through substrate
q_{conv}	convective heat flux
Q_{diss}	electrically dissipated power in the sensor
R_{arm}	electrical resistance of the active bridge arm
R_{sensor}	electrical resistance of the sensor
R_{top}	top resistance in the bridge
T_{amb}	ambient temperature
T_{sensor}	sensor temperature
T_{tube}	tube temperature
$T_{tube,0}$	tube temperature at zero flow velocity
V_{bridge}	bridge voltage
V_0	bridge voltage at zero velocity.

Greek symbol

δ	thickness of the sensor substrate.

Table 1. Turbulence levels of the wind tunnel used

Reynolds no.	Tu [%]
7050	1.60
15 100	0.67
22 300	0.46
29 650	0.34
36 650	0.34
43 250	0.29
49 350	0.34

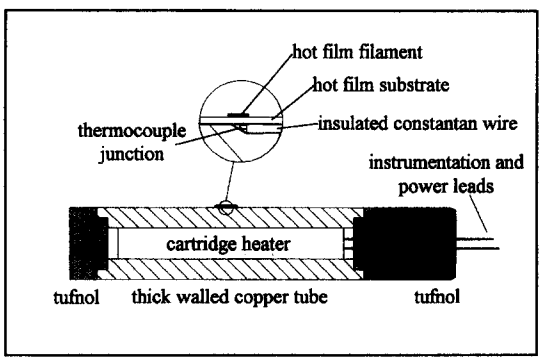

Fig. 1. Schematic of the constructed test cylinder.

consisted of a thick-walled copper tube of 25 mm diameter, with an internal cartridge heater, approximating a uniform wall temperature boundary condition. The ends of the tube were constructed of an insulating material to reduce axial heat loss. Midway along the instrumented tube length, a thin constantan wire was embedded flush with the surface, and the tip of the wire was electrically connected to the copper of the tube to form a type T thermocouple junction. A Dantec 55R47 hot film sensor was mounted directly above this thermocouple junction in such a way that the hot film itself was aligned with the axis of the cylinder, giving a spatial resolution in the circumferential direction of 0.9°. The sensor consists of a 0.1 mm × 0.9 mm sputtered film of constantan on a 7 mm × 15 mm kapton substrate. The substrate is 50 μm thick. All leads were brought out of the test section through one of the insulating end pieces. A single hot film sensor was mounted on the test cylinder and measurements at different angular locations were obtained by rotating the cylinder with respect to the oncoming flow. A schematic diagram of the test cylinder is shown in Fig. 1.

The hot film was connected to a Dantec 55M10 standard bridge which maintained the temperature of the hot film at a specified value. The constant temperature mode of operation was used for its good frequency response and for direct determination of the surface heat flux. In order to ensure stable operation of the hot film, the cartridge heater was set to maintain the tube surface temperature at around 0.5°C less than the temperature of the hot film, i.e. a sensor overheat of 0.5°C was used. This is considered to be optimal for the present set-up, as described by Scholten and Murray [13]. The temperature of the hot film, determined by monitoring the film resistance, and the surface thermocouple reading were calibrated against a reference thermometer, giving an uncertainty of ±0.3°C in each absolute temperature reading. However, the estimated uncertainty in temperature difference between the hot film and the tube surface is ±0.1°C.

The response characteristic of the sensor were determined from a square wave test, where the response time is defined as the time at which the bridge voltage has corrected for 90% of an artificially superimposed step change in the bridge electronics. From this, the frequency response has been estimated as approxi-

mately 10 kHz for a 0.5°C overheat of the hot film relative to the tube surface. This is in agreement with the results obtained by Moen and Schneider [14] for the frequency response characteristics of hot films of various dimensions and temperature differences.

For velocity measurements in the vicinity of the test tube, hot wire anemometry is inappropriate because of the temperature gradients close to the heated tube surface. Thus, laser Doppler anemometry was used. The single component laser Doppler system consisted of a 32 mW HeNe laser with Bragg cell for frequency shifting, and was used in the forward scatter mode. The photomultiplier signal was processed by a TSI 1980B counter type processor which outputs velocity data points together with the time between successive data points.

DATA ACQUISITION AND PROCESSING

The output from the wheatstone bridge and the output from the embedded thermocouple junction were logged on a Pentium P5-60 computer through 2 channels of an Amplicon PC-30PGL AtoD board. The heat flux values were then calculated by dividing the amount of electrical power dissipated in the hot film sensor (determined from the sensor/bridge set-up):

$$Q_{\text{diss}} = (V_{\text{Bridge}}^2 - V_0^2)\frac{R_{\text{sensor}}}{(R_{\text{arm}} + R_{\text{top}})^2} \quad (1)$$

by the effective surface area of the hot film. This is bigger than the geometrical surface area due to lateral conduction of heat through the substrate, as described by Beasley and Figliola [15], giving:

$$q_{\text{diss}} = \frac{Q_{\text{diss}}}{A_{\text{eff}}} \quad (2)$$

The main contribution of conduction to the tube through the sensor substrate is in the power dissipation associated with voltage V_0, which corresponds to the no flow condition. However, as the tube temperature under test conditions may differ slightly from that with zero flow, additional conduction between the sensor and tube is accounted for by use of the embedded thermocouple:

$$q_{\text{cond}} = k_{\text{kapton}}\frac{(T_{\text{tube}} - T_{\text{tube},0})}{\delta} \quad (3)$$

This is added to the heat flux originating from the dissipation of electrical energy to give the total convective heat flux as:

$$q_{\text{conv}} = q_{\text{diss}} + q_{\text{cond}} \quad (4)$$

in which the positive sign results from the definition used for the additional conduction term. The Nusselt number is then calculated as:

$$Nu = \frac{q_{\text{conv}}D}{k_{\text{air}}(T_{\text{sensor}} - T_{\text{amb}})} \quad (5)$$

The presence of the hot film sensor on the copper tube leads to local disruption of the thermal boundary layer and distortion of the Nusselt number distribution. However, a correction procedure based on the measured shear stress distribution is used to overcome this problem. Details of this correction procedure are given by Scholten and Murray [13].

Data acquisition for the combination of LDA and heat transfer rates was performed by simultaneous recording through the direct memory access technique (DMA) into the computer, and A to D conversions were started by a triggering pulse from the LDA-counter processor in such a way that a heat transfer data point is taken each time an LDA point is taken. The velocity and heat flux data, which both consist of discrete data points and time-between-data points, were resampled at equidistant time intervals by using a 1st order interpolation. This has been shown by Simon *et al.* [16] to reduce bias in spectral estimates from randomly sampled data. The average data rate for the random time spaced sampling was approximately 5 kHz for all tests, and the reconstructed data were resampled at equidistant time intervals of 2 kHz with spectra computed up to 1 kHz.

The degree of correlation between turbulence and heat flux was estimated using coherence functions rather than the usual cross-correlation function. The coherence function gives the degree of correlation as a function of frequency and is considered to provide more insight into the mechanisms of turbulent heat transfer. In addition, the phase difference between velocity and heat flux signals provides information on the heat transfer mechanisms. The auto spectra for the turbulence and heat transfer data were calculated using FFT based procedures and the coherence function, which is a normalised form of the cross spectrum (e.g. Bendat and Piersol [17]), was computed from these.

EXPERIMENTAL UNCERTAINTY

The effective surface area is the surface area modified to take account of lateral conduction and is estimated by Nusselt number calibration, i.e. the surface area is adjusted until the Nusselt numbers obtained from the measurements match relevant Nusselt numbers from the literature. A single value of effective surface area is obtained for all flow conditions. Although the resulting effective surface area is within the range quoted by Beasley and Figliola [15], this calibration process represents the main source of uncertainty in the estimate of Nusselt number. The measured Nusselt numbers are repeatable to within $\pm 2\%$ but the systematic error resulting from estimation of the effective surface area may be as high as 15%.

RESULTS

This section contains the results obtained for the cylinder in cross flow with main stream velocities

ranging from 5–35 m/s, corresponding to tube Reynolds numbers of 7190–50 350. The data are presented as plots of time-averaged Nusselt numbers together with the root mean square (rms) of the Nusselt number fluctuations as a function of angular location on the circumference. In addition, the results are presented in the form of heat transfer auto spectra and time traces. From simultaneous sampling measurements, results for the coherence and phase have been included.

Variation of local Nusselt number

Figure 2(a) shows the local variation in time averaged Nusselt number for a tube Reynolds number of 21 580. In addition, the rms level of the Nusselt number fluctuations is plotted. The local heat transfer variation exhibits the characteristic features of a minimum Nusselt number at separation (85°) followed by an increase in heat transfer in the wake region. The increase in Nusselt number up to 30°, for the uncorrected Nusselt numbers, is a result of the insulating effect of the hot film sensor substrate, referred to earlier. A correction procedure which accounts for this insulating effect, detailed by Scholten and Murray [13], has been applied and the resulting local Nusselt numbers are plotted also. The mean Nusselt number, when using the corrected values, is 103.4 as compared with a value of 91.3 from the correlation of Zukauskas [18] for the mean Nusselt number of a single cylinder in a low turbulence, low blockage cross flow. This can be seen in Table 2. This difference can be attributed in the main to the blockage ratio and turbulence levels in the wind tunnel. For the front stagnation region, it can be seen from Table 2 that the agreement between the measured Nusselt numbers and those determined from the square root of Reynolds number correlation of Squire [19] is very good. From the rms plot in Fig. 2(a) it is evident that the fluctuations at the front of the cylinder are very small, whereas the fluctuations measured over the rear of the tube are large due to extensive mixing and recirculation in the wake.

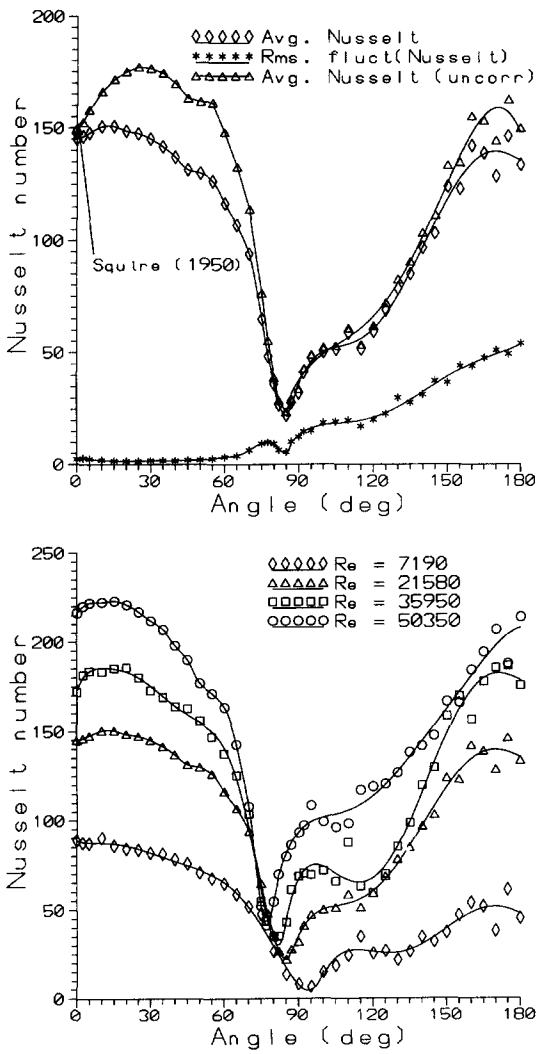

Fig. 2. Variation in local time averaged Nusselt number and Nusselt number fluctuations: (a) $Re = 21\,580$; (b) effect of Reynolds number variation.

The variation in time-averaged heat transfer with angular position is similar for the entire range of Reynolds numbers used, as can be seen from Fig. 2(b) in which the Nusselt numbers, corrected for the effect of sensor overheat, are plotted for four cases spanning the full range. It can be seen that the increasing inertial effects due to increasing Reynolds number lead to earlier separation of the boundary layer, as reflected in the movement forwards of the minimum Nusselt number position. From Table 2, it can be seen that the time-averaged Nusselt numbers agree well with data from the literature. The larger differences that are obtained for the Reynolds number of 14 380 and, to a lesser extent, 21 580 may be due in part to the blockage effect which causes a greater increase in local heat transfer when the separation point is close to 90°. Thus, although the general increase in heat transfer anticipated for a blockage ratio of 0.2 is small, Zukauskas and Ziugda [2], the measured Nusselt numbers for these cases suggests a strong increase in heat transfer at around 90°.

In Table 3, the average level of the heat transfer fluctuations is given for the Reynolds numbers used. Although the absolute magnitude of the fluctuations increases with increasing Reynolds number, it can be seen that the fluctuations, as a percentage of the average Nusselt number, decrease with increasing velocity. The one exception to this steady decrease can again be attributed to the high mean Nusselt number at the Reynolds number of 14 380.

Time traces of unsteady heat flux

In Fig. 3, time traces of the heat flux signal for the Reynolds number of 21 580 are shown for a number of angular locations on the tube surface. At 0°, small fluctuations at double the vortex shedding frequency can be observed whereas, at 5°, the fluctuations are larger in magnitude but occur only at the vortex shed-

Table 2. Comparison of average Nusselt numbers from measurements with values obtained from Zukauskas [19] and Squire [20]

Re	Nu_{fsp} (Squire)	Nu_{fsp}	% diff.	Nu_m (Zukauskas)	Nu_m	% diff.
7190	84.8	88	+3.8	47.3	49.5	+4.7
14380	119.9	129	+7.6	71.6	95.0	+32.7
21580	146.9	148	+0.7	91.3	103.4	+13.3
28760	169.6	169	−0.4	108.5	115.0	+6.0
35950	189.6	184	−3.0	124.0	127.5	+2.8
43140	207.7	210	+1.1	138.3	137.9	−0.3
50350	224.4	222	−1.1	151.7	155.1	+2.2

Table 3. Circumferentially averaged Nusselt number fluctuations and measured vortex shedding frequencies

Re	avg(Nu)	avg(rms(Nu'))	avg(rms(Nu')) [%]	Frequency [Hz]	Strouhal no.
7190	49.5	10.6	21.4	42	0.210
14380	95.0	13.5	14.2	86	0.215
21580	103.4	17.6	17.1	128	0.213
28760	115.0	19.0	16.5	172	0.215
35950	127.5	20.8	16.3	216	0.216
43140	137.9	21.2	15.4	256	0.213
50350	155.1	21.3	13.7	300	0.214

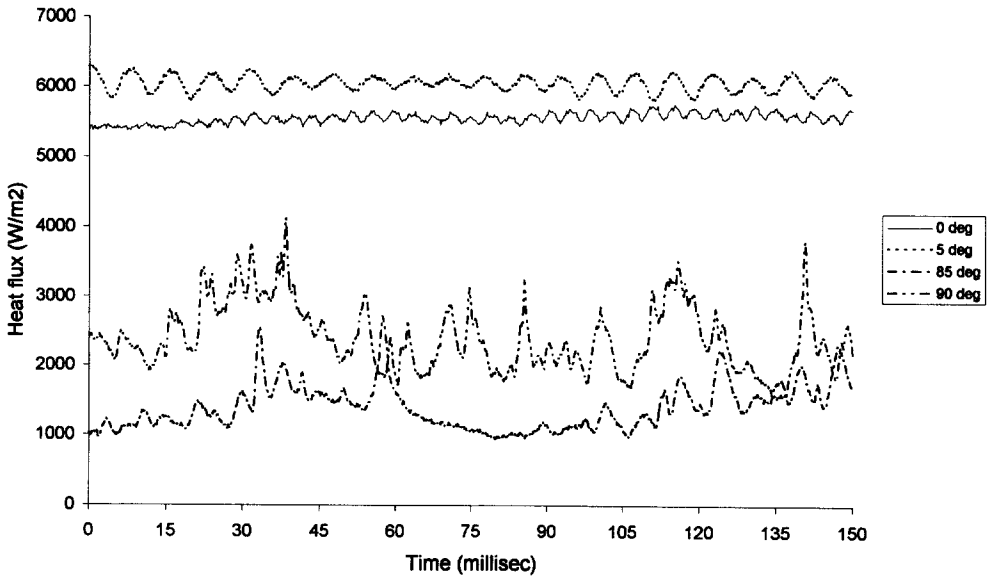

Fig. 3. Heat flux time traces, front of the cylinder, Re = 21 580.

ding frequency. The double frequency at 0° is a consequence of the oscillation of the stagnation point with respect to the hot film sensor together with the fact that the sensor signal is insensitive to flow direction. Time traces are also presented for positions immediately upstream and downstream of separation (85° and 90°). In both cases, a high content of random fluctuations is apparent, with the sudden decrease in fluctuations between 60 and 100 ms for the 85° case being characteristic of conditions immediately upstream of separation.

Heat transfer auto spectra

Figure 4(a) shows the auto spectra of the heat transfer rate, for the same Reynolds number, for three locations (0°, 5°, 80°) upstream of boundary layer separation. At the front stagnation point (0°), it can be seen that there is a large peak in the spectrum at

double the vortex shedding frequency (260 Hz). This is as expected from the time trace of heat transfer for this location, although the single frequency (130 Hz) and some harmonics are also evident. At 5°, the double frequency peak is smaller and the single frequency peak dominates. At 80°, only the single vortex shedding peak is evident, together with a general increase at other frequencies. Figure 4(b) shows the auto spectra for locations (90°, 140°, 155°) downstream of separation. It is clear that the level of high frequency fluctuations is increased dramatically, as expected from the rms of the Nusselt number fluctuations for these locations. The 140° curve is typical of the heat transfer spectra recorded in the wake; there is no evidence of periodicity in the signal. Exceptions to this exist immediately downstream of separation (90°) and at the point where the fully developed vortex from the opposite side of the cylinder impinges on the surface (155°).

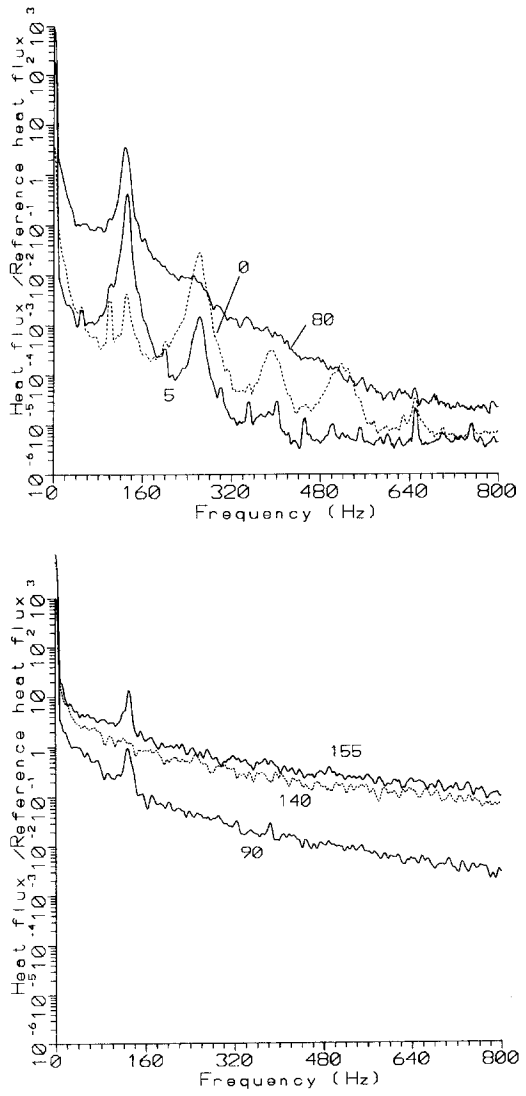

Fig. 4. Heat flux auto spectra: (a) upstream of separation, (b) downstream of separation.

Simultaneous velocity and heat transfer data

The results from the previous section indicate that the heat flux over the front of a single cylinder in cross flow is fluctuating with a frequency equal to the vortex shedding frequency. In order to gain information on the origin of these heat transfer fluctuations, measurements have been performed in which the heat transfer rate and flow velocity are measured simultaneously. Cross spectral analysis is then performed on the data obtained. The single component LDA system permits only one velocity component to be measured; the tangential velocity was selected to investigate possible correlation with the surface heat flux measurements.

For the simultaneous measurements, a location 65° from the front stagnation point was chosen as representative of locations upstream of boundary layer separation. The measurement volume of the laser Doppler system was located 1 mm from this point in the radial direction. Figure 5 shows the resulting simultaneous time records obtained for this case. It is clear that both time traces show the same trend of strong fluctuations at the vortex shedding frequency. Furthermore, at around 0.09 s into the traces, the regularity weakens considerably for both the velocity and the heat transfer rate, indicating a direct linkage between the two.

Figure 6(a) and (b) shows the auto spectra for the velocity and heat flux at 65°, with both graphs containing a strong peak at the vortex shedding frequency (130 Hz). The additional peaks evident in Fig. 6(b) originate in mains noise (50 Hz and harmonics—the second large peak is at 250 Hz, not at the double shedding frequency of 260 Hz). Figure 7(a) shows

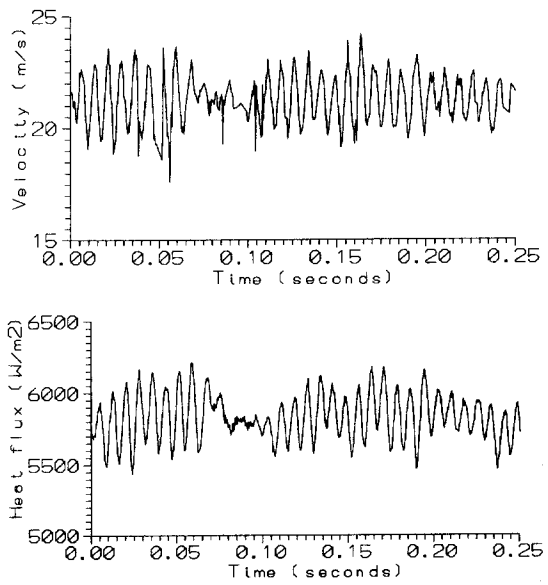

Fig. 5. Simultaneous traces of velocity and heat flux, 65°.

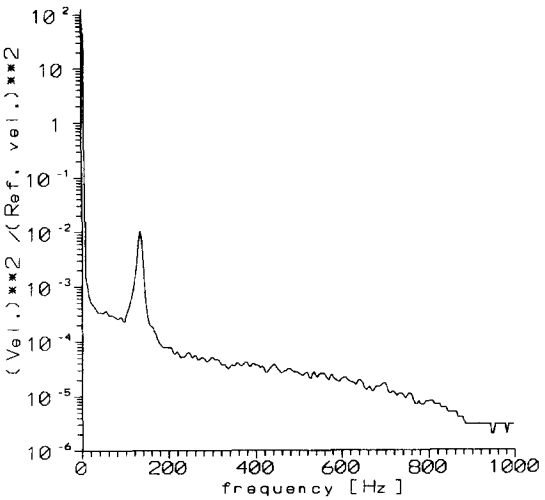

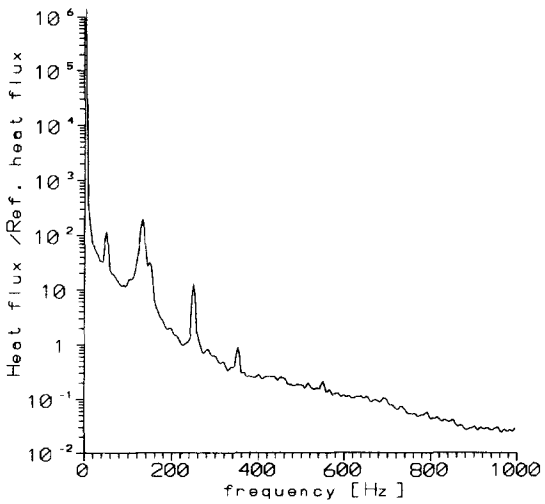

Fig. 6. Auto spectra at 65°: (a) velocity spectrum; (b) heat flux spectrum.

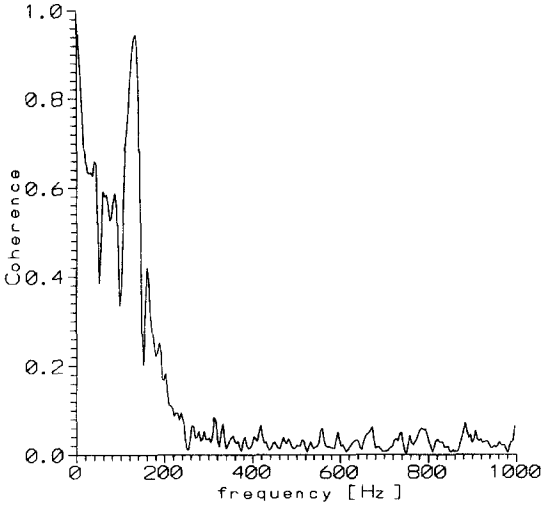

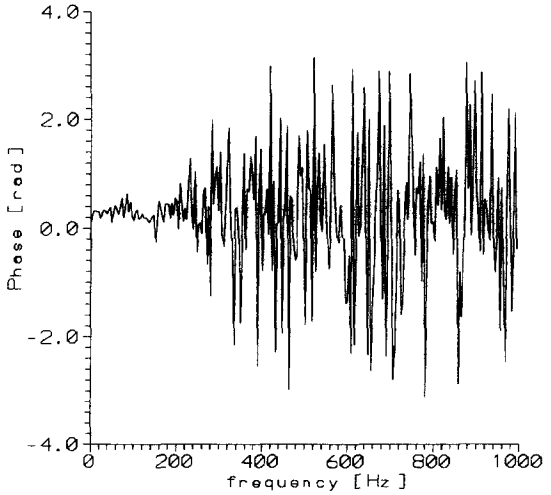

Fig. 7. Coherence and phase difference of LDA and heat flux signals, 65°: (a) coherence, (b) phase difference.

the coherence between the two signals. A maximum coherence value of 0.96 is reached for the shedding frequency, confirming the strong dependence of surface heat flux on local velocity. The low coherence for the rest of the frequency range results from the very low level of fluctuations at frequencies other than 130 Hz. Figure 7(b) shows the phase difference between the velocity and heat flux signals for this set-up. The phase difference at the vortex shedding frequency, allowing for some signal variance, is zero, indicating that there is no time delay between the velocity and heat transfer fluctuations. The significance of the measured phase difference will be addressed later.

At the back of the cylinder, the heat transfer fluctuations were found to be very large but highly random. An exception to this highly random character was found in the region around 155°, where there is some evidence of weak periodicity at the vortex shedding frequency. Figure 8 shows simultaneous time traces of heat transfer rate and velocity 1 mm from the hot film sensor, taken at 155° from the front stagnation point. It should be noted that the quality of the data obtained from measurements in this region is poor due to difficulties in seeding the flow at this location. Nevertheless, some trends can be identified. The tangential velocity shows a clear periodicity at the vortex shedding frequency as can be seen from the time trace in Fig. 8 and in the auto spectrum; Fig. 9(a). The velocity auto spectrum also shows a peak at the double shedding frequency. Figure 9(b) shows the auto spectrum of the simultaneous heat transfer data, and as in Fig. 4(b) there is a small peak detectable at the shedding frequency. This is to be expected from the time trace shown in Fig. 8, although most of the heat flux time trace consists of more random fluctuations, which is why the auto spectrum peak at vortex shedding for the 155° location is so small. Figure 10(a) shows the coherence between the measured velocity and the heat flux for the 155° position. Despite some variance in the coherence plot, a coherence value

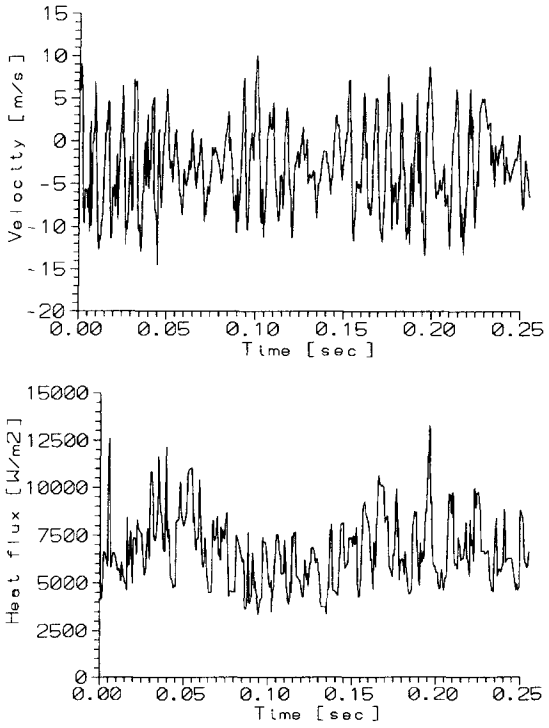

Fig. 8. Simultaneous time traces at 155°.

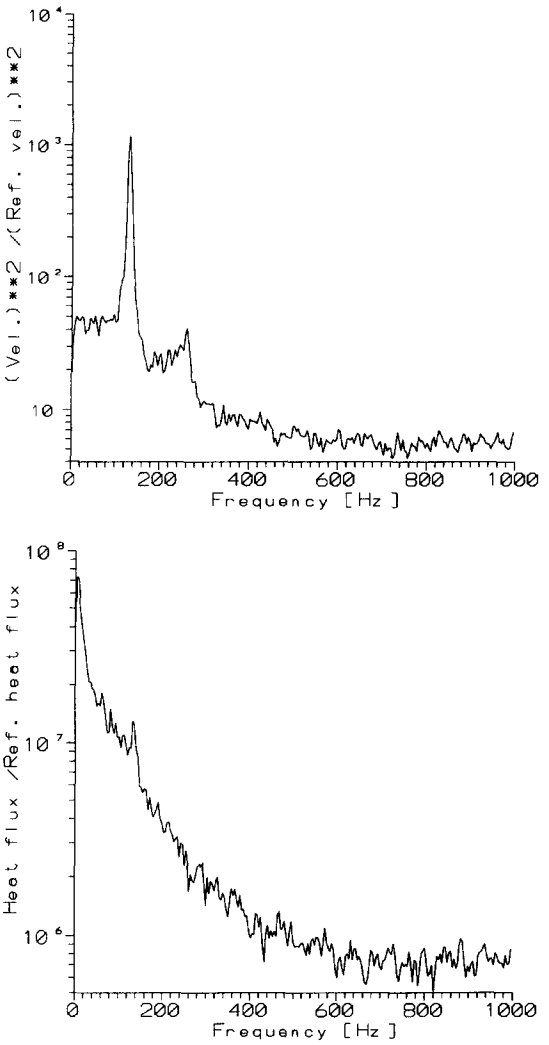

Fig. 9. Auto spectra at 155°: (a) velocity spectrum; (b) heat flux spectrum.

of 0.17 is detectable at the vortex shedding frequency, together with a very small indication of coherence at the double shedding frequency. The latter coherence suggests that the surface heat flux signal contains fluctuations at the double vortex shedding frequency, despite the absence of a peak at this frequency in the auto spectrum. The coherence levels obtained, however, are very small as compared with the values obtained for the 65° location. Figure 10(b) shows the phase difference for the 155° position. It can be seen that the phase, in contrast to that obtained for the 65° position, is highly random. This, in combination with the coherence plot, shows that the surface heat flux and the tangential velocity at 155° are very poorly correlated. An explanation for this poor correlation in the wake is given in the next section.

DISCUSSION

When the fluctuations in velocity at 1 mm from the surface at 65° are considered, it is apparent that they are linked to the growth and subsequent shedding of vortices at the back of the cylinder. This phenomenon is governed by the fact that a growing vortex imposes a larger resistance to the flow on its own side of the cylinder, thus reducing the flow velocity on that side. At the opposite side, where the growing and shedding of vortices is in anti-phase, the local flow velocity increases in order to maintain a constant mean flow. The implication of this is that the entire flow field pulsates, even in front of the cylinder, as a consequence of the formation and shedding of vortices at the back. Confirmation that the velocity fluctuations originate in a pulsating flow field can be obtained from Fig. 11(a) which shows the phase difference between surface heat flux at 65° and velocity measured 15 mm from the surface at 90°. It can be seen that the phase difference is again zero, confirming that the velocity outside the wake region changes everywhere at the same time. The coherence value for this distant measurement, at the vortex shedding frequency, equals the value obtained from Fig. 7 for the local velocity measurements. Further confirmation of the above mechanism can be found from a simultaneous test in which the surface heat flux at 65° is measured together with the velocity outside the wake at 90° at the opposite side of the cylinder. The coherence between surface heat flux and velocity, at the vortex shedding frequency, is again very high, but the phase plot shows anti-phase between the two measured entities, as can be seen from Fig. 11(b). The deviation from an exact phase difference corresponding to anti-

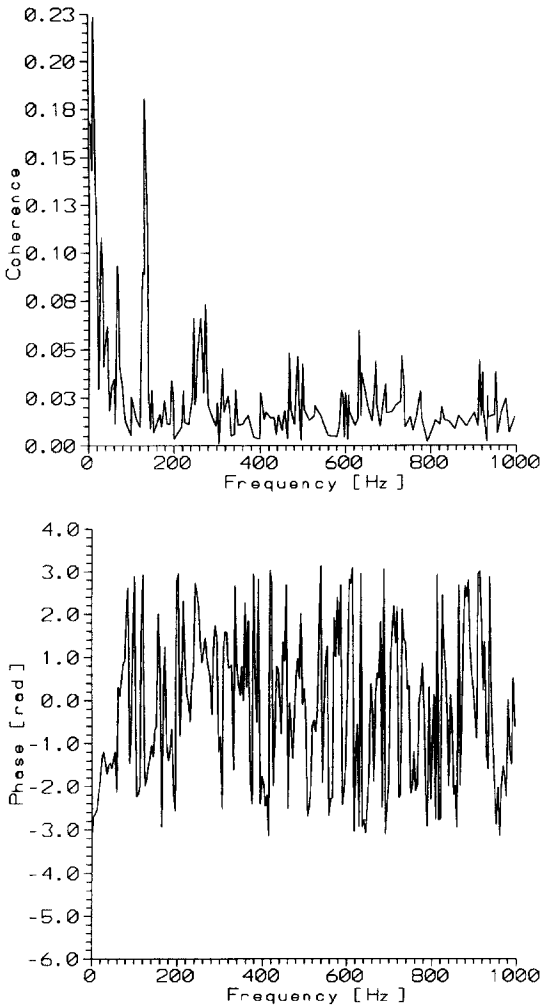

Fig. 10. Coherence and phase difference of LDA and heat flux signals, 155°: (a) coherence; (b) phase difference.

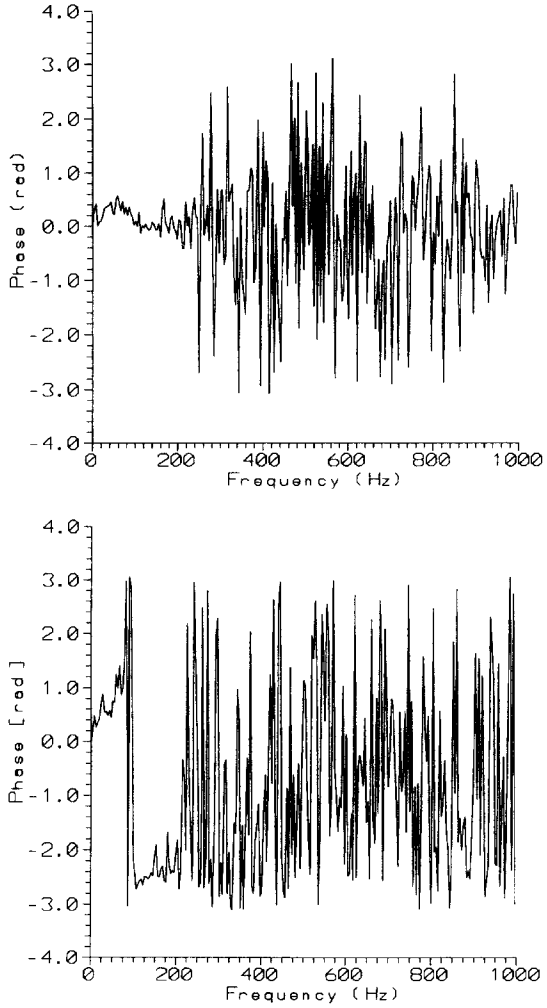

Fig. 11. Phase difference with varying LDA measurement locations: (a) measurement volume distant from the surface; (b) measurement volume at opposite side of cylinder.

phase (−3.14 radians) originates in the spectral analysis routines, which have difficulty in deciding whether the velocity leads or lags the heat transfer data. This difficulty is enhanced by some signal variance, and by using an average of spectral analysis performed on separate blocks of data, corresponding to the block length needed by the FFT routines.

For the wake region, the 155° location was described by Gerrard [20] as the location where a fully developed vortex from the far side of the cylinder contacts the surface, before separating and being transported away in the wake. It is thus possible that at this location the heat flux is maximum when the measured tangential velocity is close to zero. For the 155° location, it is likely that the normal velocity component makes a big contribution to the heat transfer rate. Furthermore, in the wake, fluid which has been heated by the upstream section of the cylinder surface is being recirculated, suggesting that the instantaneous surface heat transfer rate will depend on the fluid temperature field also. These factors may contribute to the low coherence obtained between tangential velocity and heat flux at the 155° position.

CONCLUSIONS

A method has been developed for making simultaneous measurements of time-resolved velocity, using laser Doppler anemometry, and local heat flux, using a hot film sensor, at the surface of a cylinder in cross flow. From the measurements obtained for a single cylinder in a cross flow with low freestream turbulence levels, the following conclusions can be drawn:

1. The magnitude of fluctuations in heat transfer at the front of the cylinder is very small, whereas the magnitude of fluctuations over the rear of the cylinder is very high due to the extensive mixing of fluid within the wake.
2. For the front of the cylinder, the heat transfer rate varies periodically with a frequency equal to the

vortex shedding frequency, with the exception of the front stagnation region where the fluctuations occur at twice the vortex shedding frequency. For the rear of the cylinder, the heat transfer fluctuations are more random in nature, with the exception of locations immediately downstream of separation and in the region around 155°, where there is again some evidence of periodicity at the vortex shedding frequency.

3. From the results of simultaneous velocity and heat flux tests it can be concluded that the origin of the heat transfer fluctuations at the front of the cylinder in a low turbulence cross flow lies within the pulsating character of the flow field in this area. This pulsing of the flow in front of the cylinder is a consequence of the formation and shedding of vortices at the back and causes the heat flux over an entire side of a cylinder to vary simultaneously with the flow.
4. For the wake region of a cylinder, simultaneous measurements show that the local tangential velocity and the surface heat flux are poorly correlated, indicating dependence of the local heat flux on the normal velocity component as well as on other physical quantities, for example, the fluctuations in the local temperature of the flow field as a result of recirculation of the fluid.

Acknowledgement—The authors appreciate the assistance of Prof. J. A. Fitzpatrick with the spectral analysis procedures.

REFERENCES

1. Morgan, V. T., The overall convective heat transfer from smooth circular cylinders. *Advances in Heat Transfer*, 1975, **11**, 199–264.
2. Zukauskas, A. and Ziugda, J., *Heat Transfer of a Cylinder in Cross Flow*. Springer-Verlag, 1985, pp. 97–127.
3. Murray, D. B. and Fitzpatrick, J. A., Heat transfer in a staggered tube array for a gas-solid suspension flow. ASME *Journal of Heat Transfer*, 1991, **113**(4) 865–873.
4. Scholten, J. W. and Murray, D. B., Influence of direction of heat flow on Nusselt numbers for a gas-particle cross flow. ASME *Journal of Heat Transfer*, 1995, **117**(4), 1088–1090.
5. Rosicskowski, J. and Hollworth, B., Local and instantaneous heat transfer from a isothermal cylinder in a cross flow. In *Fund. Exp. Meas. in Heat Transfer*, ASME HTD 179, 1991, pp. 49–56.
6. George, G. H., Instantaneous local heat transfer coefficients and related frequency spectra for a horizontal cylinder in a high temperature fluidised bed. *Int. J. Heat Mass Transfer*, 1993, **36**, 337–345.
7. Katoh, Y., Miyamoto, M. and Kohno, A., The study on unsteady heat transfer around a horizontal heated tube surface in a fluidised bed. *Proc. Int. Conf. On Multiphase Flows*, Tsukuba, Vol. 1, 1991, pp. 317–320.
8. Rottger, H. K. and Renz, U., Measurements of instantaneous local heat transfer coefficients around a tube immersed in a high temperature fluidised bed. *Proc. 10th Int. Heat Transfer Conference*, Brighton, Vol. 2, 1994, pp. 285–290.
9. Simmons, S. G., Hager, J. M. and Diller, T. E., Simultaneous measurements of time-resolved surface heat flux and freestream turbulence at a stagnation point. *Proc. 9th Int. Heat Transfer Conference*, Vol. 2, Hemisphere, 1990, pp. 375–380.
10. Ching, C. Y. and O'Brien, J. E., Unsteady heat flux in a cylinder stagnation region with high freestream turbulence. In *Fund. Exp. Meas. in Heat Transfer*, ASME HTD Vol. 179, 1991, pp. 57–66.
11. Meyer, K. E. and Larsen, P. S., LDA study of turbulent flow in a staggered tube bundle. *7th Int. Symposium on Applications of Laser Anemometry to Fluid Mech.*, Lisbon, 1994, pp. 39.4.1–39.4.7.
12. Balabani, S., Bergeles, G., Burry, D. and Yianneskis, M., Velocity characteristics of the crossflow over tube bundles. *7th Int. Symposium on Applications of Laser Anemometry to Fluid Mech.*, Lisbon, 1994, pp. 39.3.1–39.3.7.
13. Scholten, J. W. and Murray, D. B., Measurement of convective heat transfer using hot film sensors: correction for sensor overheat. ASME *Journal of Heat Transfer*, 1996, **118**(4), 982–984.
14. Moen, M. J. and Schneider, S. P., The effect of sensor size on the performance of hot-film sensors. ASME *Journal of Heat Transfer*, 1994, **116**, 273–277.
15. Beasley, D. E. and Figliola, R. S., A generalised analysis of a local heat flux probe. *J. Physics E*, 1988, **21**, 316–322.
16. Simon, L., Scholten, J. W. and Fitzpatrick, J. A., Velocimetrie laser: amelioration du traitement des donnees experimentales par interpolation d'ordre 1. *Congris Francais de Mecanique*, Strasbourg, 1995, pp. 321–324.
17. Bendat, J. S. and Piersol, A. G., *Random Data Analysis and Measurement Procedures*, Wiley Interscience, New York, 1986.
18. Zukauskas, A., Heat transfer from tubes in cross flow. *Advances in Heat Transfer*, 1972, **8**, 93–160.
19. Squire, H. B., *Modern Developments in Fluid Dynamics*, 3rd edn, Vol. 2, Clarendon Press, Oxford, 1950.
20. Gerrard, J. H., The mechanics of the formation region of vortices behind bluff bodies. *J. Fluid Mechanics*, 1966, **25**(2), 401–413.